

Performance comparison of passive control schemes for the numerically improved ASCE cable-stayed bridge model

Marco Domaneschi* and Luca Martinelli^a

Department of Structural Engineering, Politecnico di Milano, Milano, Italy

(Received June 1, 2011, Revised September 30, 2011, Accepted December 5, 2011)

Abstract. The benchmark on the ASCE cable-stayed bridge has gathered since its proposal the interest of many specialists in the field of the structural control and the dynamic response of long span bridges. Starting from the original benchmark statement in the MATLAB framework, a refined version of the bridge model is developed in the ANSYS commercial finite element environment. A passive structural control system is studied through non linear numerical analyses carried out in time domain for several seismic realizations in a multiple support framework. An innovative electro-inductive device is considered. Its positive performance is compared with an alternative version considering traditional metallic dampers.

Keywords: cable-stayed; bridge; passive; control; user-element; earthquakes

1. Introduction

Social growth and economic transformation: this is probably the main role long span bridges actually play, becoming themselves strategic buildings. Their protection against external hazards, as seismic events, is essential. Structural control can offer useful solutions contributing to the stability and safety of such structures (Spencer *et al.* 2003).

Starting from the original framework of the benchmark (Caicedo *et al.* 2003), this work deepens the results of previous investigations (Bontempi *et al.* 2003, Casciati *et al.* 2008, Domaneschi 2010) which retained the cable-stayed bridge model, originally developed in a simplified version into the MATLAB environment.

Herein, a refined model of the bridge is studied using the ANSYS commercial finite element (FE) code (Ansys Release 11.0) which has proven capable of the implementation of structural control systems and dynamic simulation of complex long span bridges (Ubertini and Domaneschi 2006, Hong *et al.* 2009, Domaneschi and Martinelli 2011). The advances include new aspects in: (I) the simulation of the stay cables dynamics, with respect to the coupled motion with the main girder, (II) in the implementation of the seismic excitation, (III) in the soil-structure interaction and (IV) in supporting the outcomes resulting from the previous investigations of the original benchmark statement with respect to the efficiency of passive control strategies.

This last aspect is pursued explicitly considering the spatial variability of the seismic input for

* Corresponding author, Lecturer, E-mail: domaneschi@stru.polimi.it

^a Assistant professor: luca.martinelli@polimi.it

several seismic realizations, to comprise a statistical approach to the bridge response.

A passive structural control system is considered by implementing on the bridge model an innovative electro-inductive device (Casciati and Domaneschi 2007). Its positive performance is compared with an alternative version considering traditional metallic dampers.

The electro-inductive device is modeled by means of an ANSYS hysteretic element. For comparison purposes, and to extend the capabilities of modeling different classes of control dampers, a new passive element, which adopts the Bouc-Wen model (Wen 1976, Casciati and Faravelli 1991) as its constitutive law, is developed for the simulation of metallic-damper devices. The Bouc-Wen model has been proven reliable and is widely adopted for structural control applications in bridge engineering. This new solution is coded into an external program which exchange data with the main ANSYS procedure; details on this implementations are given herein also.

2. The cable-stayed bridge

2.1 The structure

The cable-stayed bridge proposed in the control benchmark (Caicedo *et al.* 2003) is an existing fan-type cable stayed bridge: the Bill Emerson Memorial Bridge (Fig. 1), located near Cape Girardeau (Missouri, USA), spanning the Mississippi River (on Missouri 74-Illinois 146 roads), designed by the HNTB Corporation (Hague 1997). Seismic considerations entered design of the bridge due to the bridge site (the New Madrid seismic zone) and its role as a principal crossing of the Mississippi River. The governing loading case for the design was determined to be due to seismic effects.

Various designs were considered, including full longitudinal restraint at the towers or no longitudinal restraint. Due to temperature effects, it was found that fully restraining the deck in the longitudinal direction would result in unacceptably large stresses while incorporating force transfer devices, between the towers and the deck, would provide the most efficient solution. Sixteen 6.67 MN shock transmission devices are employed in the longitudinal direction to allow for expansion of the deck due to temperature changes. Under dynamic loads these devices are assumed to behave as rigid links. In the transverse direction earthquake restrainers are employed at the connection between the tower and the deck, while the deck is constrained in the vertical direction. The bearings at bent 1 and pier 4 (Fig. 1) are designed to permit rotations about the transverse and vertical axis and thermal longitudinal displacements.

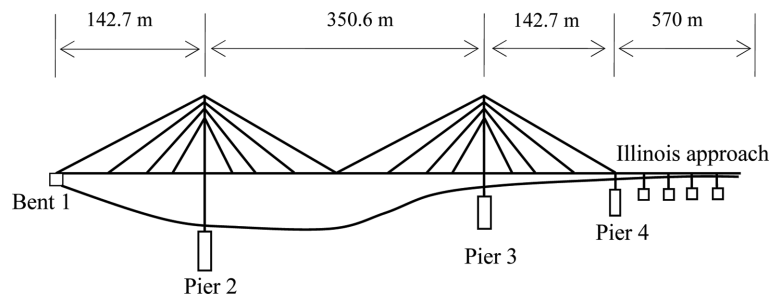


Fig. 1 Bridge scheme

2.2 The bridge model

Part of the original benchmark focused on the bi-directional horizontal nature of the seismic excitation. Soil-structure interaction was not considered since the foundations of the bridge are on the bedrock. The same ground motion was applied at each support, considering only the time delay due to the finite velocity of waves propagation. The numerical model did not consider nonlinearities during the time history analysis, apart from the control system the participants would propose. More details about this issue are reported in (Caicedo *et al.* 2003).

In this paper a more general and refined numerical approach is studied which considers the vertical component of the earthquake as well. Furthermore, the seismic input is not the same on all the supports but a coherence function of literature is introduced so as to have different signals satisfying a fixed correlation function. The soil type regulates the correlation degree (lagged coherency).

The model comprises soil-structure interaction through the use of impedance functions (Sieffert and Cevaer 1992, Fogazzi and Perotti 1998), the piers and bents foundations are simulated by lumped masses with soil-equivalent springs and dampers.

The original benchmark statement does not consider degrees of freedom for the cables beside those of the extreme nodes, neglecting their modal and dynamic description. Focusing the attention on the simulation of the structural dynamics, the cable model is refined moving from the single rod type representation to a description with six rope elements for each cable. The adopted ANSYS cable element was previously tested in a tensioned setting, similar to that of the bridge stay cable, and the results were in good agreement with an analytical approach based on the transfer functions and Irvine's theory (Ubertini and Domaneschi 2006). A detailed description of the improvements adopted in the ANSYS refined version of the original benchmark statement are reported herein.

3. Multiple-supports input and soil-structure interaction

The equations of motion of a soil-structure system subjected to multiple-support seismic excitation can be written in matrix form as

$$\mathbf{M}\ddot{\mathbf{q}} + \mathbf{C}\dot{\mathbf{q}} = \mathbf{R} + \mathbf{Q}_s + \mathbf{Q} \quad (1)$$

where \mathbf{q} is the vector of Lagrangian coordinates (representing the total generalized displacements), \mathbf{M} and \mathbf{C} are the inertia and damping matrices, while \mathbf{R} , \mathbf{Q}_s and \mathbf{Q} are vectors listing, respectively, the generalized components of the non-linear restoring forces, of the equivalent seismic forces and the other dynamic forces. A dot denotes derivative with respect to time. If we assume linear behavior of the ground and lumped parameters (frequency independent) modeling of soil-structure interaction, the seismic term can be expressed as

$$\mathbf{Q}_s = \begin{bmatrix} 0 \\ \mathbf{C}_{cc}^{(g),(f)} \dot{\mathbf{q}}_c \end{bmatrix} + \begin{bmatrix} 0 \\ \mathbf{K}_{cc}^{(g),(f)} \mathbf{q}_c \end{bmatrix} \quad (2)$$

Where $\mathbf{q}_c(f)$ is the vector listing the free-field ground displacement at the soil-structure contact

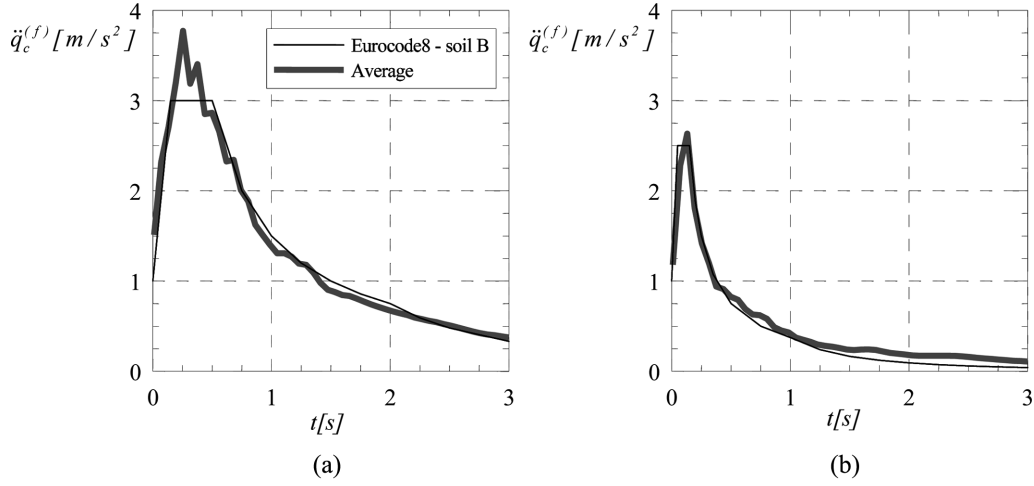


Fig. 2 Average pseudo-acceleration spectrum, computed from 10 realizations of the ground motion, and Eurocode 8 elastic spectrum for the horizontal (a) and vertical (b) component

points, while $C_{cc}(g)$ and $K_{cc}(g)$ are respectively the soil damping and stiffness matrices referred to the free-field ground velocities and displacements at the contact points. The simulation of free-field ground displacements is presented in the next section.

4. Simulation of the seismic motion

In this work, the free-field ground displacements $q_c^{(f)}$ and velocities $\dot{q}_c^{(f)}$ have been obtained from synthetic generated acceleration time histories, considering the spatial variability of the seismic ground motion. The last is a complex phenomenon involving several factors, among these are the “wave-passage”, “extended source”, “scattering” and “local” effects, which induce non negligible consequences on large structures.

The acceleration time histories are obtained by the procedure presented in (Monti *et al.* 1996), which relies on the spectral representation method by (Shinozuka 1972). At all stations, the generated accelerations satisfy the well known Kanai-Tajimi Power Spectral Density, as modified by (Clough and Penzien 1975). The statistical differences between the motions at different stations satisfy the coherency function proposed by (Luco and Wong 1986); a velocity of the shear waves $v_s = 3000$ m/s and an incoherency factor $\alpha = 0.2$ has been adopted.

The parameters of the Clough and Penzien power spectral density (PSD) have been chosen (Martinelli *et al.* 2011) in order to minimize the difference between the value of the median response pseudo-acceleration spectrum with that given by (Eurocode 8). Fig. 2 compares the average pseudo-acceleration spectrum, computed from 10 realizations, with that of (Eurocode 8) for the horizontal and vertical component, respectively.

5. Structural control strategy

A passive control system has been adopted. This consists in 16 devices distributed along the

bridge axis in both longitudinal and transversal direction. The devices, which connect the deck with the piers and bents, are located under the bridge deck symmetrically with respect to the bridge longitudinal axis (Fig. 3(a)). The devices allow the bridge to dissipate energy both in the longitudinal and transversal directions. Eight devices work in the longitudinal direction, the remaining in the transversal one. They are intended to work in series with the original shock transmission elements which have the role of absorbing the low velocity deformations resulting from the thermal loads. Fig. 3(b) shows a detail of the structural control devices configuration.

The dampers are characterized by an hysteretic behavior descending from a symmetric elastic and perfectly plastic constitutive law having yielding force $F_y = 1000$ kN and Young modulus $E = 80000$ kN/m. These parameters are selected according to previous investigations (Bontempi *et al.* 2003, Domaneschi 2010).

The hysteretic control devices are first simulated in the framework of the ANSYS code by a non linear unidirectional element (“combin39”) with elastic-plastic force-deflection capability (Ansys

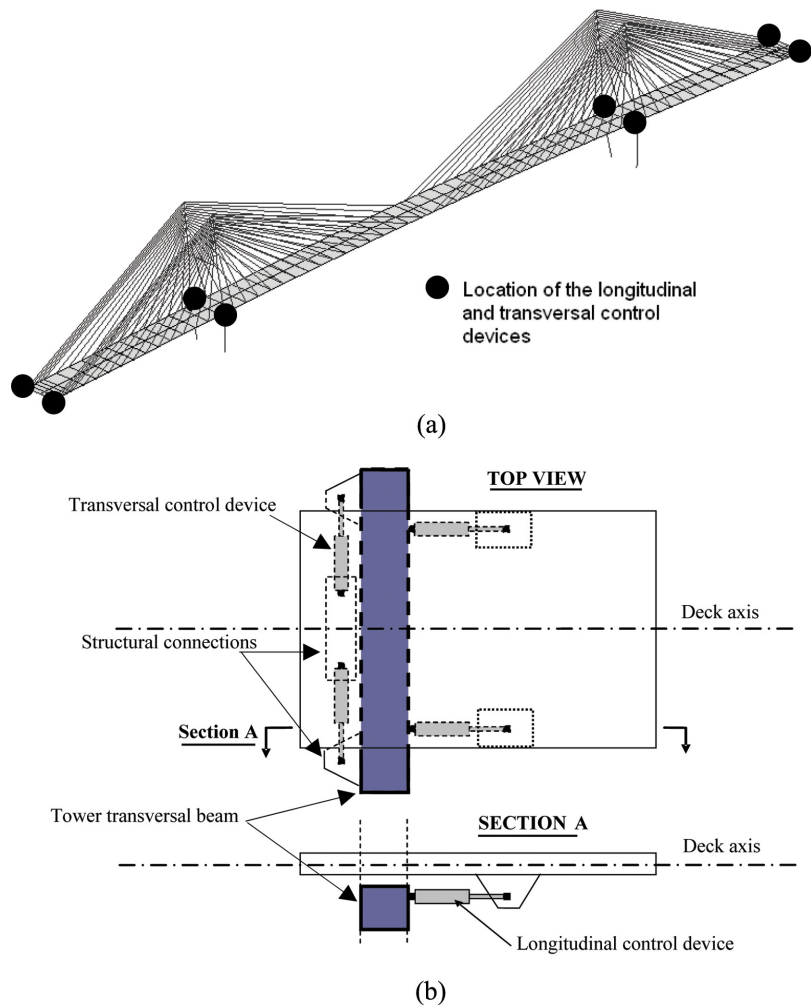


Fig. 3 FE mesh and passive control devices location: whole model (a), connection detail (b)

Release 11.0). This is a uniaxial tension-compression element with three degrees of freedom at each node: translations in the nodal x , y and z directions. No bending or torsion is considered. It is worth to underline that the elastic-plastic characteristic for the devices of the control strategy here investigated closely reflects the performance of an electro-inductive device prototype, tested in laboratory (Casciati and Domaneschi 2007). In this respect this numerical research supports future useful implementations in real bridge structures.

Subsequently, to broaden the class of damping devices, the Bouc-Wen endochronic hysteretic model (Wen 1976) has been adopted for the control devices. The Bouc-Wen model has been often selected for the simulation of dissipative passive and semi-active devices, such as metallic dampers, rubber bearings, piezoelectric dampers (Low and Guo 1995), magneto-rheological dampers (Spencer *et al.* 1997) and electro-inductive devices (Casciati and Domaneschi 2007). The choice to idealize passive and semi-active devices by the Bouc-Wen law is supported by the physical and mathematical consistency of that model (Erlicher and Point 2004) and the excellent correspondence between the experimental and numerical results.

In particular it has been demonstrated (Ikhouane *et al.* 2005, 2007) as an appropriate choice of its parameters makes the Bouc-Wen model capable of describing a passive behavior, in that it does not create energy, and able to reproduce the free oscillations of a system subject only to inhomogeneous initial conditions. This, and the fact that the model is stable in reproducing a limited response to a limited input, makes the Bouc-Wen model ideal for the simulation of passive semi-active control elements. The ability of such model in the simulation of control systems with different characteristics (like passive, semi-active and hybrid) is also very attractive in a multipurpose work frame.

In the remaining of this section a procedure is presented for implementing in the ANSYS environment a control element which constitutive law is the Bouc-Wen one.

6. Implementation of the Bouc-Wen model in ANSYS

In the ANSYS environment it is possible to implement a user-element to perform a behavior not already contained in the libraries of the commercial code. The default path, however, requires the development and the validation of a new ANSYS executable which contains the new component the user wishes to implement. This requires the user to (a), understand the interfacing routine provided by the ANSYS code, (b), correctly guess how the parameters passed to this routine should actually be used at the different stages of execution (element state determination at sub-steps, element state update, etc.), (c), gather the software tools (compiler, debugger, linker) required for building the specific ANSYS version on the selected hardware platform.

An alternative that ameliorates these troubles without requiring a re-link of the ANSYS executable, is simply to write a program external to ANSYS and dialogue with it through interface files, read and written using routines developed in the powerful APDL (Ansys Parametric Design Language) (Domaneschi *et al.* 2009, 2010). This has the advantage that the validation of the external program and the APDL procedures, only, is required since the ANSYS executable remains unchanged. Following this second path, the implementation of a passive control user-element is presented, which adopts the Bouc-Wen law. The element has been subsequently used as an alternative to ANSYS combin39 element on the cable-stayed bridge model.

6.1 Bouc-Wen model

According to the Bouc-Wen endochronic hysteretic model, the equations governing the restoring force produced in a passive device, which connects two points, are given as

$$\dot{z} = A\dot{x} - \beta\dot{x}|z|^n - \gamma|\dot{x}|z|^{n-1} \quad (3)$$

$$\Phi(x, t) = (1 - \alpha)kz + \alpha kx + c\dot{x} \quad (4)$$

where z is an auxiliary variable controlling the hysteretic behavior, x and \dot{x} are the relative displacement and velocity, respectively, between the device end-nodes and $\Phi(x, t)$ is the device control force. A , β , γ , n and α are time invariant parameters defining, respectively, the amplitude of the cycles, the shape of the cycles, the linearity in the unloading, the smoothness of the transition from the pre- to the post-yield region, the ratio between post and pre-yielding stiffness.

The control force is expressed as the sum of three terms, representing different sub-elements acting in parallel. The viscous damping component, which is due to the damping coefficient c , is practically very small, and it is neglected in the presented formulation. The control force, Φ_y , at yielding assumes the following form whenever $A=1$ and α is close to zero (Casati and Faravelli 1991)

$$\Phi_y = \frac{k}{(\beta + \gamma)^{1/n}} \quad (5)$$

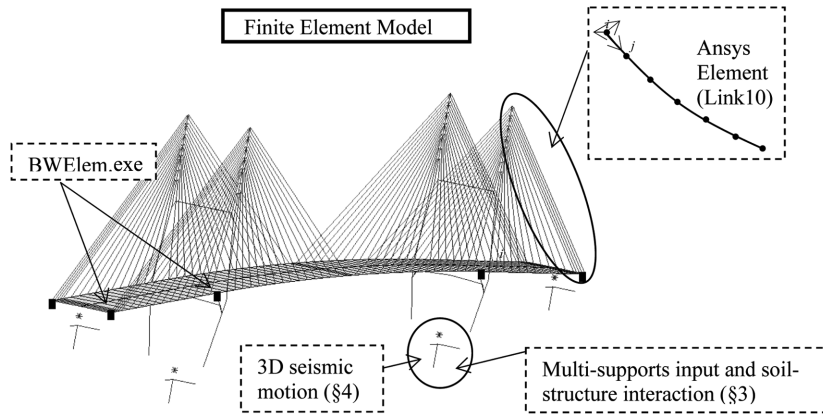
6.2 Implementation

The simulation of an element with a constitutive law given by the Bouc-Wen model (which will hereafter be briefly denominated Bouc-Wen element) requires, with the proposed procedure, the implementation of a Fortran executable, "BWElem.exe", that, at each step of analysis is called by the script governing the ANSYS analysis. The procedure is carried out writing APDL routines capable of extracting the kinematics of the nodal points joined by Bouc-Wen elements, write appropriate interface files, call the external executable, read and then apply to the structural model the externally computed control forces. In particular, the process of calling the external executable from the ANSYS script was carried out using the APDL command "/SYS" (Ansys Release 11.0). Fig. 4(a) depicts the bridge scheme implemented in the Ansys script with the new features. Once the numerical model in study is defined in the input list of ANSYS, the procedure requires that commands to perform the following steps be issued:

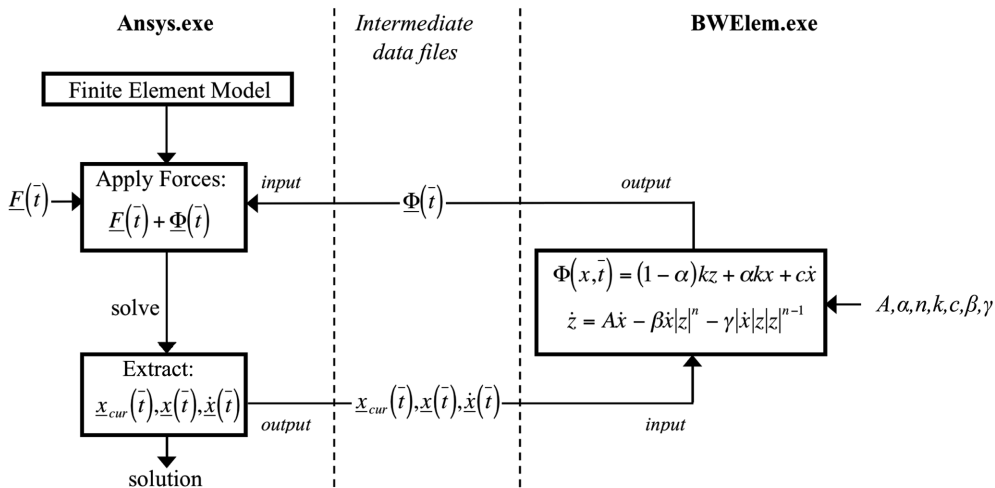
- extraction at the end of each step \bar{i} of analysis of the current positions $\underline{x}_{cur}(\bar{i})$, displacements $\underline{x}(\bar{i})$ and velocities $\underline{\dot{x}}(\bar{i})$ of the nodes connected by Bouc-Wen elements, expressed in the ANSYS global frame of reference;
- writing of these quantities in appropriate interface files;
- execution of the external program BwElem.exe through the command /SYS;
- extraction of the control forces $\underline{\Phi}(\bar{i})$ from the interface files compiled by the external executable, and application for pass $\bar{i}+1$ of the same with the external forces $\underline{F}(\bar{i}+1)$ at the nodes connected by Bouc-Wen elements.

The operations carried out by BwElem.exe can be summarized in the following steps:

- acquisition for each element of the model parameters $A, \alpha, \beta, \gamma, n$ and k ;
- acquisition of nodal kinematical parameters $\underline{x}_{cur}(\bar{t}), \underline{x}(\bar{t}), \dot{\underline{x}}(\bar{t})$, in the overall frame of reference of ANSYS;
- determination from $\underline{x}_{cur}(\bar{t})$ of the orientation of each Bouc-Wen element, in the ANSYS global frame of reference;
- reading of the status at the end of the previous analysis step (or initialization of the state for the first step of analysis) and integration of the hysteretic variable z in Eq. (3). This latter operation is performed using the adaptive Runge Kutta method RK45 which couples two Runge Kutta methods, respectively the fourth and fifth order using the coefficients of Cash and Karp;
- determination of the nodal control forces of the Bouc-Wen model in the local reference of every element, and transformation in the global ANSYS reference, therefore. Subsequent writing of the forces thus determined in interface files.



(a)



(b)

Fig. 4 Scheme of the finite element model (a) and flowchart of the implemented procedure (b)

The above described procedure is illustrated by the block diagram in Fig. 4(b), relative to the analysis step at time \bar{t} . ASCII interface files are used for the data flow purpose. In the same picture, $\underline{E}(t)$ symbolically denotes the read operation of the forces into the ANSYS environment while A , α , n , k , c , β and γ the read of the constants characteristic of each Bouc-Wen element into the BwElem.exe executable.

The procedure thus implemented involves the decoupling between determination of the structure equilibrium from the state determination of each Bouc-Wen element. Particularly, the procedure requires that the control forces are computed with BwElem.exe from the kinematics extracted in ANSYS at the end of step \bar{t} while they will be applied to the structure only at the beginning of step $\bar{t} + 1$. This aspect will be the object of the following section.

6.3 SDOF System and the Bouc-Wen user-element

The delay in computing the control forces has a twofold effect: first it implements, in principle, a slightly different control strategy; secondly it can affect the precision in the integration of the endochronic equations (Eq. (3)). These will be studied with reference to a SDOF oscillator, having a short (0.31 s) period to enhance the errors effects, by comparing the results with those coming from a MATLAB implementation of SDOF dynamics.

The proposed user-element is applied to the single degree of freedom (SDOF) system in Fig. 5, where a mass $m = 200 \text{ kNs}^2/\text{m}$ is connected to an elastic spring of stiffness $k_s = 1000 \text{ kN/m}$ and to a passive control element of the Bouc-Wen type.

The relative displacement of the mass m , and hence of Node 2, with respect to the reference is x_2 while $a_x(t)$ is the acceleration of the reference system. Node 1 connects mass m to the reference through an elastic spring while Node 3 links m to the reference through a passive Bouc-Wen element, characterized by the parameters in Table 1. The coupled system of equations controlling

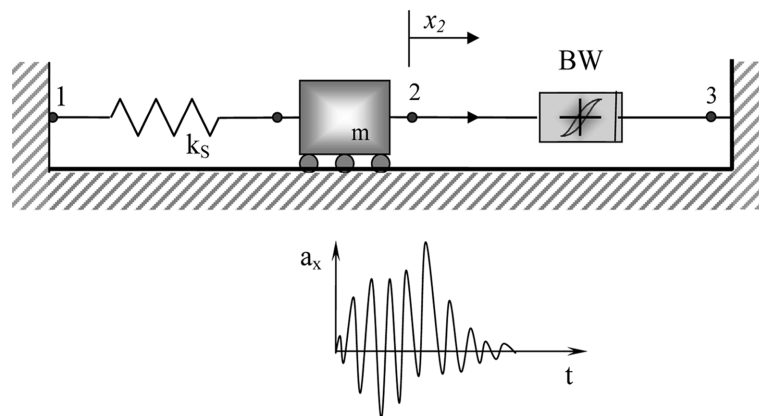


Fig. 5 SDOF system under seismic excitation controlled with a passive Bouc-Wen element

Table 1 Parameters of the passive Bouc-Wen model

A	N	α	$\beta \text{ (m}^{-1}\text{)}$	$\gamma \text{ (m}^{-1}\text{)}$	$k \text{ (kN m}^{-1}\text{)}$	$\Phi_y \text{ (kN)}$
1	1	0.02	60	60	80000	666.7

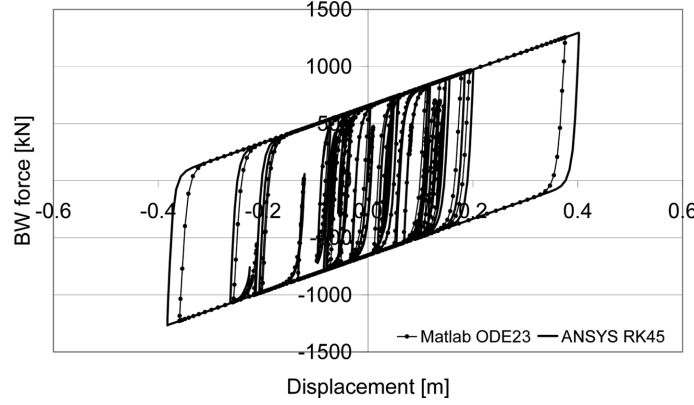


Fig. 6 Hysteretic cycles for the passive Bouc-Wen model

the problem is then the following

$$m(\ddot{x}_2 + a_x) + k_s x_2 + [ak(x_2) + (1-a)kz] = 0 \quad (6)$$

$$\dot{z} = A\dot{x}_2 - \beta\dot{x}_2|z|^n - \gamma|\dot{x}_2|z|z|^{n-1} \quad (7)$$

$$\dot{x}_2(t=0) = x_2(t=0) = 0 \quad (8)$$

Comparison between the ANSYS code, using the implemented procedure BwElem.exe, and the MATLAB solution is provided by following steps:

- solution in MATLAB of the coupled system of ODE in Eqs. (6-8) and determination of the force and displacement x_2 for the Bouc-Wen element;
- implementation of the same dynamic oscillator in ANSYS by finite elements and adopting the here proposed approach for computing externally the hysteretic contribution;
- comparison of the forces obtained with the two different procedures.

Fig. 6 reports the hysteretic cycles obtained by ANSYS with BwElem.exe and the MATLAB procedures using in both cases a time integration step $dt = 0.01$ s. As it can be seen, the solutions computed are equivalent, with less 5% of a difference in terms of displacements.

7. Development of the bridge model

The finite element mesh consists in about 2600 nodes and 2800 elements. These are linear beam elements for towers and the deck frame, linear shells for the concrete deck slab, and tension-only truss elements for the stay cables. Each cable is divided into 6 “Link 10” elements. The materials are characterized by linear elastic behavior: concrete for the piers; high-strength, low-relaxation steel for the cables. The composite structure of the deck (steel frame with concrete slab) is accurately modeled by concrete shell elements connected to steel beams. The two materials retain their individual characteristics.

A small structural damping, equal to 3% of the critical one, is implemented through a Rayleigh type damping computed between the first and the sixth mode to ensure reasonable values for the

Table 2 Modal identification vs the benchmark statement

Mode	Frequency [Hz]		Period [s]		Shape	
	Benchmark	ANSYS	Benchmark	ANSYS	Benchmark	ANSYS
1	0.289	0.289	3.46	3.46	Vertical symmetric	Vertical symmetric
2	0.369	0.368	2.71	2.72	Vertical anti-symmetric	Vertical anti-symmetric and longitudinal
3	0.468	0.428	2.14	2.34	Torsional symmetric	Torsional symmetric
4	0.515	0.564	1.94	1.77	Torsional anti-symmetric	Torsional anti-symmetric
5	0.581	0.612	1.72	1.63	Vertical symmetric	Vertical symmetric
6	0.649	0.64	1.54	1.56	Lateral and torsional symmetric	Lateral and torsional symmetric
7	0.668	0.672	1.50	1.49	Not specified	Vertical anti-symmetric and longitudinal
8	0.697	0.73	1.43	1.37	Not specified	Vertical symmetric
9	0.71	0.736	1.41	1.36	Not specified	Torsional symmetric
10	0.72	0.772	1.39	1.30	Not specified	Torsional anti-symmetric

damping ratios for the modes contributing significantly to the seismic response ($\alpha_R = 0.075$ and $\beta_R = 0.0103$ respectively the mass and stiffness matrix multipliers).

Using impedance function, soil-structure dynamic effects are accounted for by inserting elastic springs (in the vertical, transversal and longitudinal direction, respectively for translational and rotational degrees of freedom) at each foundation (bents and piers); viscous dashpots are provided as well, acting in parallel to springs. Computation of the stiffness and damping constants is based upon the instruction reported in (Sieffert and Cevaer 1992). The foundations masses are accounted for by a lumped nodal mass: element “mass21” in (Ansys Release 11.0).

7.1 Validation: static and modal analysis

The uncontrolled configuration, equivalent to the real bridge structure, is implemented establishing the equilibrium on the deformed configuration, with the mass density of structural materials and the gravitational acceleration. The resulting displacements field is corrected by tensioning the 64 cables using different thermal expansion coefficients (depending on the cable length) with a constant temperature variation. Using this procedure it is possible to rearrange the nodal positions in the overall model, reaching the bridge configuration specified on the design including the initial stress state induced by the mass density.

This procedure allows to correctly reproduce the original numerical model in the new analysis framework, as the results presented in Table 2 confirm. These refer to a modal analysis used for the identification of the bridge dynamics. The modal analysis (Lanczos method) was performed after the static one, so that the effects of self-weight and of cable pre-tensioning are included in the structural stiffness matrix (Ansys Release 10.0).

8. Results: structural control for seismic input

The bridge is studied by means of non-linear time history analyses in the uncontrolled and

controlled configuration in the case of seismic loading. The geometry and the boundary conditions suggest to perform the transient analyses also in large displacements with the seismic input time histories. It follows that the relation between displacements and strains in the structure is non-linear and the solution is determined by the full Newton Raphson iterative method (Ansys Release 11.0).

The results of this section show the bridge response during realizations of a 20 s long seismic input. They start from achievement of the static equilibrium configuration for the structure, at time $t = 70$ s. Results pertaining to the initial time interval of 70 s correspond to application of self-weight and cable pre-tensioning and are omitted.

8.1 Extension of the benchmark results

The extension of the benchmark problem is carried out in terms of the statistical results of the bridge response for five seismic sets of a 20 s long seismic input. Starting from the refined version of the bridge model, and adopting the established improvements in terms of seismic loads simulation and structural behavior, the ANSYS elastic-plastic combin39 element is used for implementing the passive control strategy on the structure.

Following (Clough and Penzien 1975), the components of the 3D earthquake acceleration can be considered as uncorrelated; hence, each set of seismic input is formed by paring at the support points acceleration histories belonging to three different realizations, two for the horizontal directions (oriented as the global horizontal axes) and one vertical. Moreover, histories in the same direction differ from one support to another, but satisfy the chosen coherence function and, on average, the EC8 spectrum.

The mean and standard deviation of the extreme values over five seismic input sets, are considered, as well as the maximum and the minimum values. Table 3 reports such mean statistical variables computed over five seismic input sets. It is worth noting as the internal actions are generally mitigated by the control system, in particular the standard deviation is strongly reduced. Also the extreme values of the shear and bending moment at the tower base show a useful

Table 3 Mean on five seismic sets [m kN] (x longitudinal axis, y transversal horizontal, z vertical)

Bridge response	Uncontrolled				Controlled			
	MEAN	STD	MAX	MIN	MEAN	STD	MAX	MIN
Deck mid span: displacement X	-0.0031	0.0311	0.0790	-0.0801	-0.0108	0.0458	0.0957	-0.1275
Deck mid span: displacement Y	-0.0010	0.0425	0.0999	-0.1076	-0.0070	0.0418	0.0939	-0.1249
Deck mid span: displacement Z	0.0005	0.0218	0.0479	-0.0465	0.0028	0.0216	0.0534	-0.0435
Tower top: displacement X	-0.0037	0.0388	0.0975	-0.1017	-0.0116	0.0521	0.1134	-0.1470
Tower top: displacement Y	-0.0016	0.0298	0.0973	-0.1010	-0.0015	0.0226	0.0780	-0.0745
Tower top: displacement Z	0.0004	0.0030	0.0058	-0.0072	0.0004	0.0030	0.0057	-0.0071
Tower base: shear X	3667	6837	21346	-13242	398	1592	5595	-6154
Tower base: shear Y	11440	3635	25658	-1209	11359	2222	20252	2879
Tower base: bending moment (Y axis)	42966	74447	286795	-225504	43147	47776	202749	-119488
Tower base bending moment (X axis)	75427	153738	471563	-306210	5613	41641	119763	-135949
Cable tension	3726	150	4085	3334	4000	134	4311	3650

decrement. According to the passive control theory of seismic effects, these positive results come at the cost of a small increment of the structural displacements. The tension of the cables has been also investigated in the controlled and uncontrolled configurations without showing significant variations from the values under static loads, this outcome has been also found in (Domaneschi 2010) analyzing the solution in the original benchmark statement.

Figs. 7 and 8 report some significant results in terms of time histories and power spectral densities

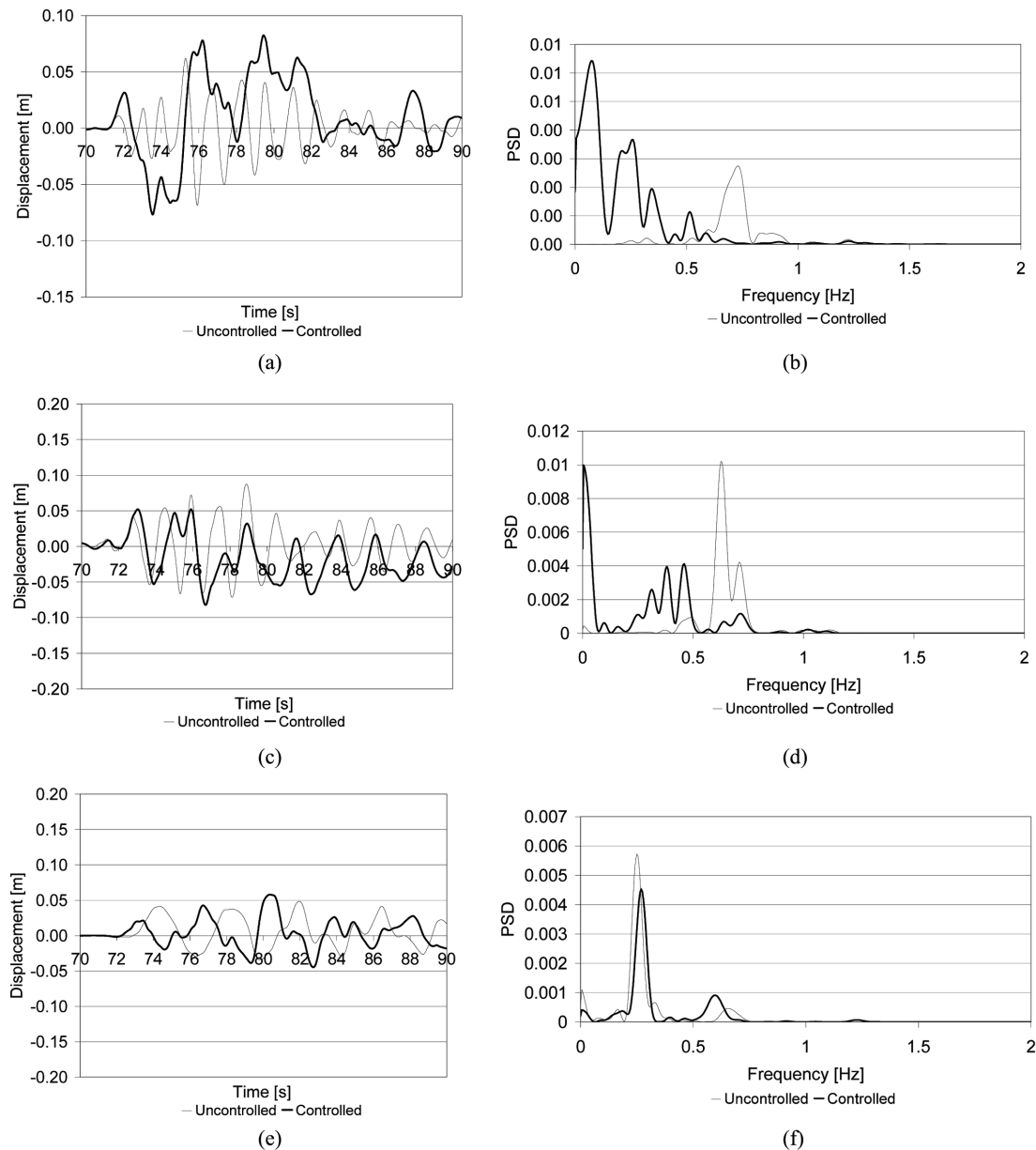


Fig. 7 Displacement time histories (left) and linear PSD (right) at the deck mid span for seismic set 1; bold line controlled, thin line uncontrolled, for direction x (a, b), y (c, d) and z (e, f)

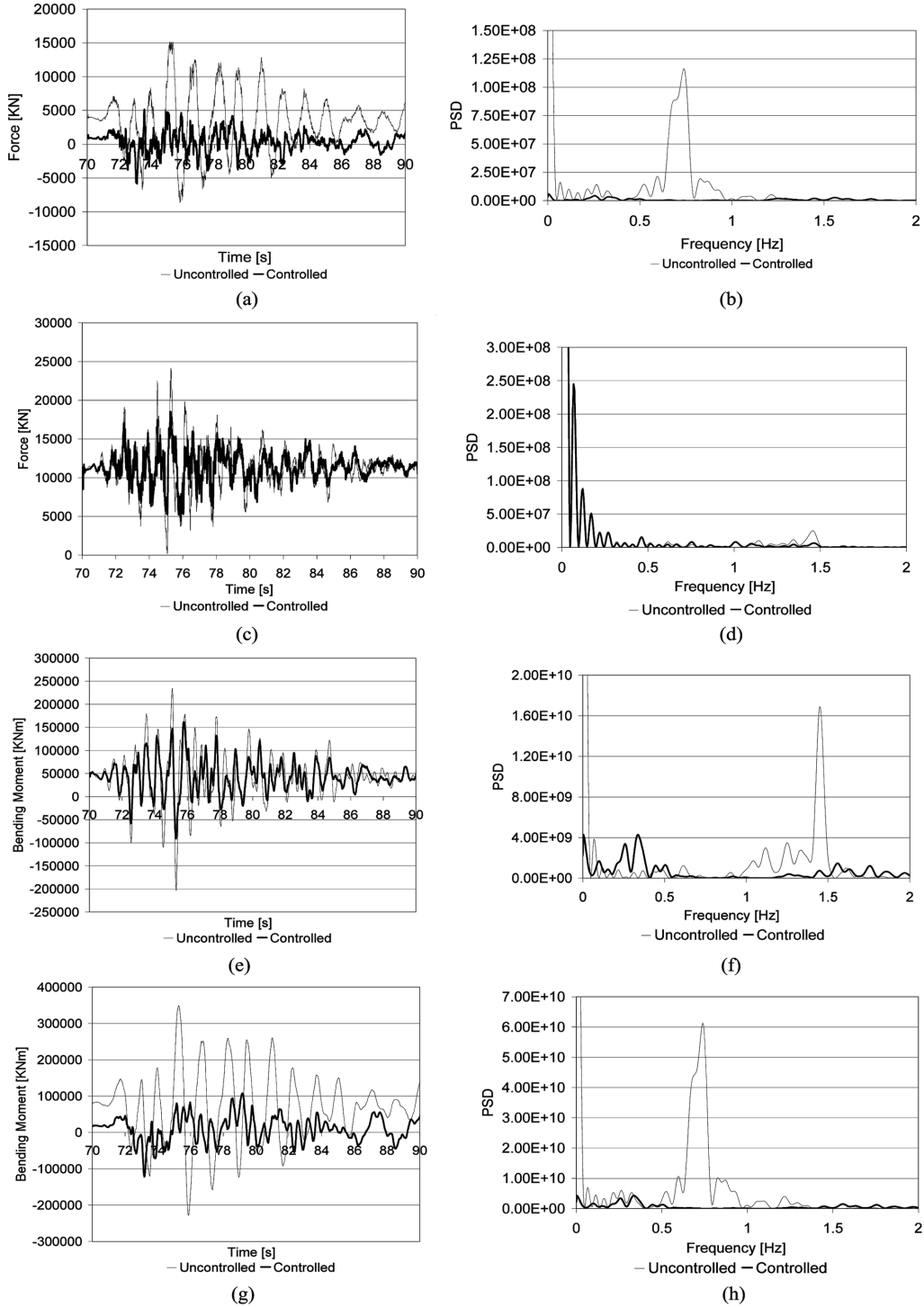


Fig. 8 Shear force and bending moment time histories at the tower base (left) and linear PSD (right) for seismic set 1; bold line controlled, thin line uncontrolled. Force in direction x (a, b), in direction y (c, d); bending moment around axis x (e, f) and axis y (g, h)

(PSDs) evaluated by the periodogram approach (Oppenheim and Shafer 2010). The structural response is firstly represented by the displacements in longitudinal, transversal and vertical directions, xyz axes respectively, at the deck mid span (Fig. 7). In time domain the extreme value of the structural response for the controlled case remain equivalent to the uncontrolled one, and sometimes is slightly increased (Fig. 7(a)). The vertical displacements are more similar since less affected by the dissipative devices.

The frequency content of the horizontal component shows however very interesting differences (Figs. 7(b), (d)): the controlled case is characterized by larger values of the lower frequencies. The uncontrolled structural system tends to behave as a stiffer structure (the difference between these two configuration is yielding of the horizontal connection elements between the deck and towers and bents). Its dynamic behavior tends to amplify higher frequency components of the earthquake shaking. The passive control system, based on an hysteretic response, protects the bridge by: (a) acting as an internal fuse for the forces applied by the deck to the supports, (b) shifting the structural response to lower frequencies and, (c) dissipating a much larger part of the seismic energy introduced into the structural system. These good outcomes are clearly represented in Fig. 8. The internal actions (shears and bending moments) at the piers base are evidently mitigated (Figs. 8(a), (c), (e), (g)), in particular in the longitudinal direction. The frequency analysis of such responses underlines lower amplitudes characterized also by lower frequencies.

It is worth noting that the natural frequencies of the bridge in the uncontrolled configuration, as listed in Table 2, can be readily identified in the PSD periodograms with a reasonable correspondence (e.g. in Figs. 7(b), (d), (f)).

A representative hysteretic behavior for the control devices applied on the bridge model between the deck and towers in longitudinal and transversal direction, simulated by the ANSYS elastic-plastic element *combin39*, is reported by the cycles of Fig. 9(a) (seismic set 1). As it can be seen, the longitudinal device dissipates more seismic energy if compared to the transversal one (as it is also clarified in Fig. 9(b)). However the latter is still effective in dissipating energy. This observation is in agreement with the conclusions of previous investigations in the original framework (Casciati *et al.* 2008, Domaneschi 2010).

The device cycles in Fig. 6(a) reproduce identically those by an innovative electro-inductive device characterized in laboratory for structural control applications on long span bridges (Casciati and Domaneschi 2007). They represents a fascinating solution for the feasibility of larger devices of this type to be installed in long span bridges. This is very interesting due to two facts: that they are much shorter than hydraulic dampers of identical maximum stroke and that they can be easily converted into the semi-active type, adapting themselves to different seismic intensity levels (Domaneschi 2010) by using simple open-loop control laws. An additional aspect to be underlined of such semi-active devices is the self-centering ability after a seismic event, realigning the deck with the piers and the bents. In this light, the presented results are also intended as a realistic validation of such control strategies on a cable-stayed bridge by using an accurate model of the structure and of the loading conditions.

8.2 Alternative version of the damping devices

The previously cited electro-inductive device is an interesting solution for the control of large structures. It is not however already available on the market. In this section the alternative solution of using metallic dampers will be presented. This device type has been commercially available since

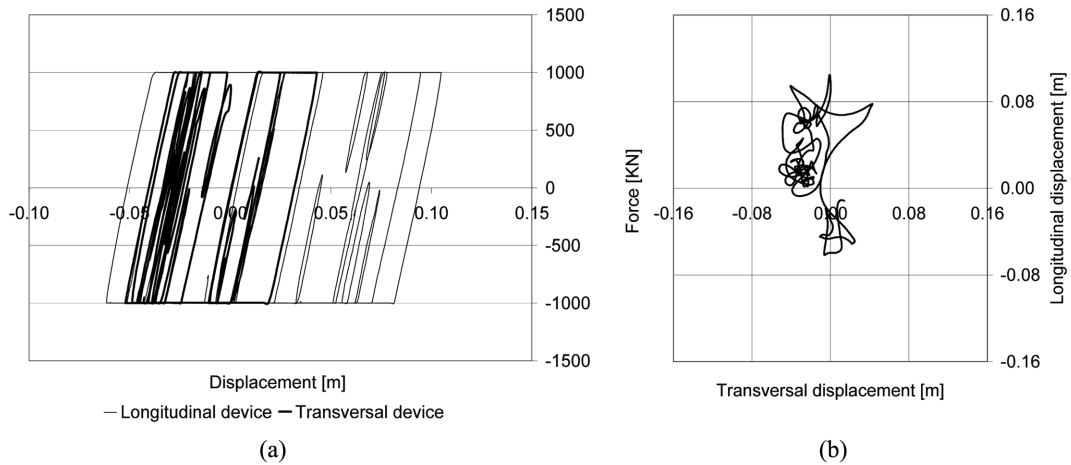


Fig. 9 Hysteresis cycles in longitudinal and transversal direction for seismic set 1 of the ANSYS elastic-plastic element at the tower -bold line transversal, thin line longitudinal- (a) Deck relative displacements (b)

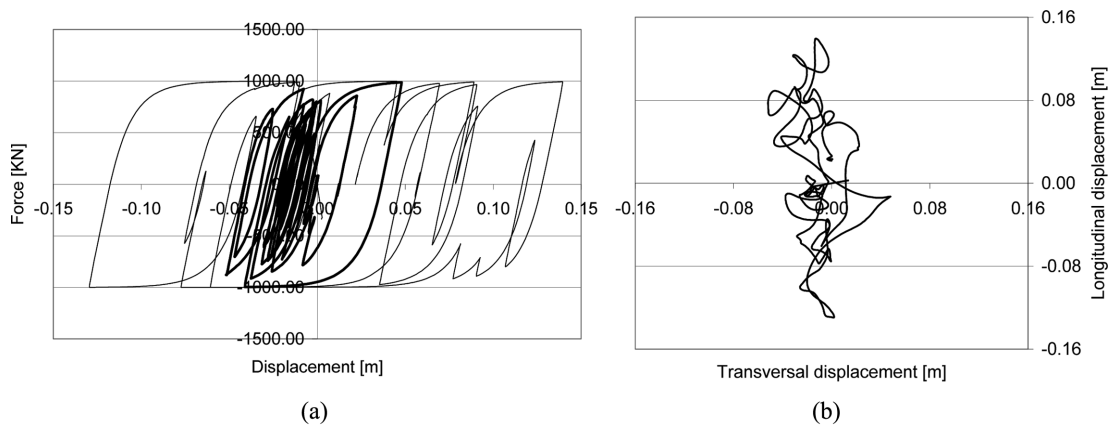


Fig. 10 Hysteresis cycles in longitudinal and transversal direction for seismic set 1 of the Bouc-Wen element at the tower -bold line transversal, thin line longitudinal- (a) Deck relative displacements (b)

several years, now.

The elastic-plastic transition in the hysteretic characteristic of the vast majority of metallic dampers is smoother than that of the previously cited electro-inductive device, so a more adaptable numerical model is necessary for correctly simulating such behavior. In light of this consideration, the Bouc-Wen user-element described in Section 6 is adopted for investigating in a consistent way the effectiveness of structural control schemes utilizing metallic dampers. In the remaining of this section, the performance of the bridge control system which uses metallic dampers will be presented. The comparison with the electro-inductive solution is discussed.

For the seismic input set 1, Fig. 10 depicts the hysteresis cycles performed by the Bouc-Wen elements ($A = 1$, $\beta = \gamma = 40$ [m⁻¹], $n = 1$, $\alpha = 0.001$, $k = 80000$ [kNm⁻¹]) reacting in the transversal and longitudinal direction at the tower. It can be compared with Fig. 9 where the cycles performed by the ANSYS element combin39 are reported. It is worth noting a good agreement between the two control responses, even if the Bouc-Wen elements show slightly higher displacements due to

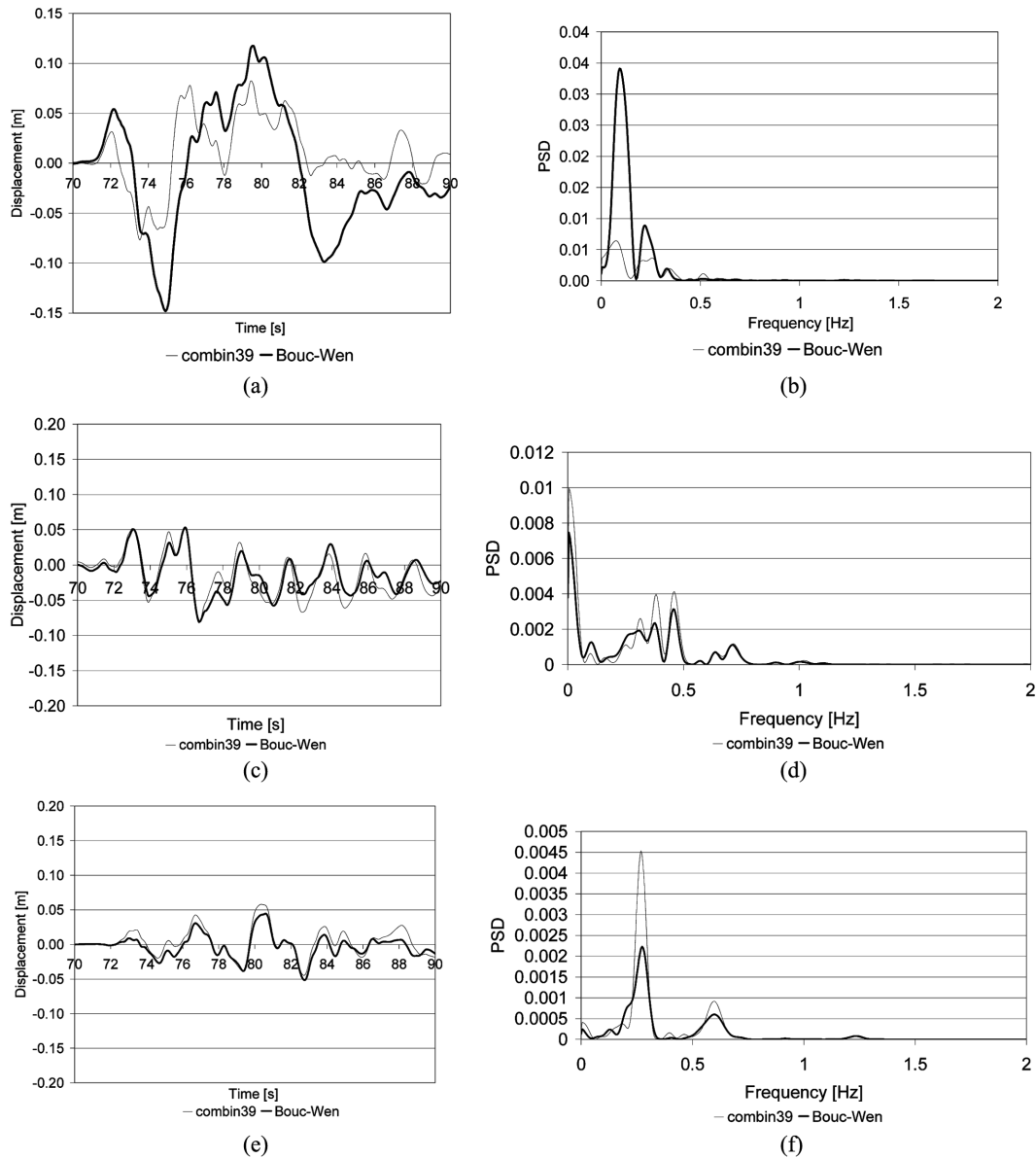


Fig. 11 Displacement time histories and linear PSD at the mid deck (seismic set 1, bold line Bouc-Wen): x (a, b), y (c, d) and z direction (e, f)

the lower stiffness in the elastic-plastic transition. In this simulation it can be also seen how the longitudinal device dissipates more seismic energy if compared to the transversal one. It can be concluded as such behavior is, as a matter of fact, independent from the characteristics of the hysteretic passive devices.

Fig. 11 shows the time histories and the PSD periodograms of the displacements at the deck mid span. In time domain coincident responses are obtained but for the longitudinal displacement, where the Bouc-Wen device allows a larger movement of the deck. The investigation in the frequency

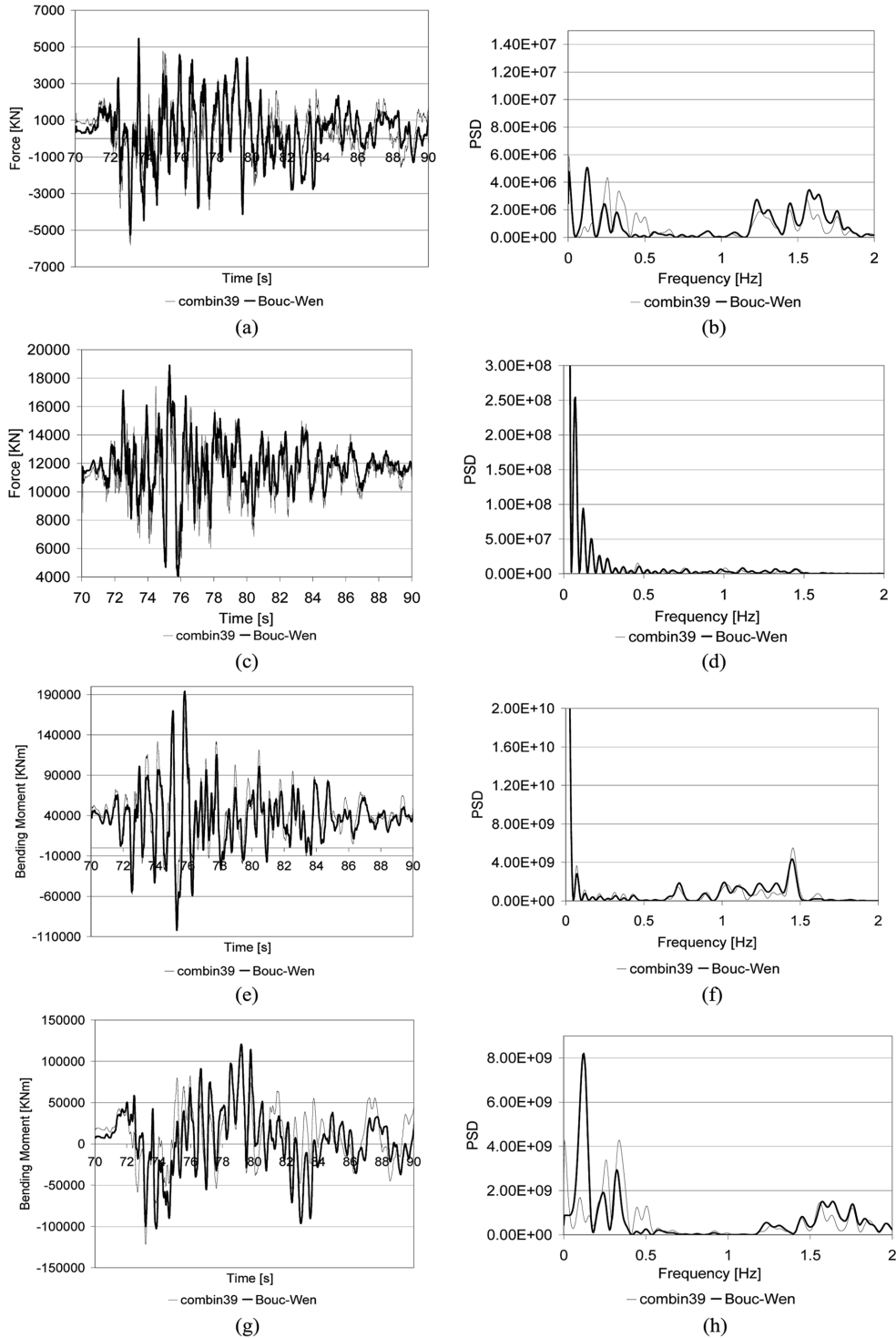


Fig. 12 Shear time histories and linear PSD at the tower base: x (a, b), y (c, d) directions. Bending moment: around x (e, f) and y (g, h) directions. Seismic set 1, bold line Bouc-Wen

domain (Figs. 11(b), (d), (f)) highlights these aspects: the bridge main frequencies for both control system are equivalent, but the combin39 and the Bouc-Wen model perform the largest relative displacements in different directions: respectively in transversal-vertical direction and in the longitudinal direction.

The internal actions at the tower base are reported in Fig. 12. Time histories are comparable for both the control systems while some minor differences appear in the frequency domain. Analysis of internal action time histories points out that the positive beneficial effects highlighted for the electro-inductive devices can be extended also to the metallic-dampers.

9. Conclusions

A refinement of the ASCE bridge benchmark model is studied inside the ANSYS commercial finite element code including new modeling aspects in the numerical simulation, namely: the soil-structure interaction, the seismic excitation, the geometric non linearity and the cables dynamics. Passive control devices are firstly implemented by an ANSYS element into a verified control scheme, referring to a laboratory tested electro-inductive prototype. The multi support dynamic excitation consists in five seismic sets of records applied to the bridge. The effect of the structural control consists in the dissipation of the seismic energy and in the shift of the bridge main natural frequencies toward lower values with respect to the uncontrolled configuration of the bridge. The positive contribution of the dissipative devices in the longitudinal and transversal directions, in the mitigation of the seismic effects, arises from the analyses in terms of internal actions and displacements. These last are sometimes moderately increased, this is in accord with the passive control theory.

An innovative user-element is linked to the refined bridge model. It adopts the Bouc-Wen model as its base and, distinctively, it is coded in an external stand-alone computer program. Such element is able to simulated different families of control devices and it has been used to investigate the bridge response when the control system implements metallic dampers. The obtained results are in good agreement with those coming from the ANSYS element.

This conclusion corroborates the work in the original benchmark, developed using a less refined structural model, and achieves more general results on the application of passive devices on cable-stayed bridges.

Acknowledgements

This work has been partially supported by MIUR (Ministry of Education, University and Research) under the project "Dynamic response of linear and nonlinear structures: modelling, testing and identification" (PRIN 2009).

The authors wish to acknowledge Prof. F. Perotti for his discussions and support in the field of dynamic of structures, which along with his guidance have been essential in the development of the refined numerical model. Michele Romano performed the validation analyses of the ANSYS user-element, in partial fulfillment for the requirements of the Bachelor's Degree in Civil Engineering at Politecnico di Milano, under the guidance of the authors. His contribution is also acknowledged.

References

- Ansys Academic Research, Release 11.0, Ansys Inc, USA.
- Bontempi, F., Casciati, F. and Giudici, M. (2003), "Seismic response of a cable stayed bridge: active and passive control systems (Benchmark problem)", *J. Struct. Control*, **10**(3-4), 169-185.
- Caicedo, J.M., Dyke, S.J., Moon, S.J., Bergman, L., Turan, G. and Hague, S. (2003), "PhaseII benchmark control problem for seismic response of cable stayed bridges", *J. Struct. Control*, **10**(3-4), 137-168.
- Casciati, F., Cimellaro, G.P. and Domaneschi, M. (2008), "Seismic fragility of a cable-stayed bridge when retrofitted by hysteretic devices", *Comput. Struct.*, **86**, 1769-1781.
- Casciati, F. and Domaneschi, M. (2007), "Semi-active electro-inductive devices: characterization and modelling", *J. Vib. Control*, **13**(6), 815-838.
- Casciati, F. and Faravelli, L. (1991), *Fragility analysis of complex structural systems*, Taunton, Somerset, England, Research Studies Press Ltd.
- Clough, R.W. and Penzien, J. (1975), *Dynamics of structures*, McGraw-Hill, New York, N.Y.
- Domaneschi, M. (2006), "Structural Control of Cable-stayed and Suspended Bridges", Ph.D. Thesis, Università degli Studi di Pavia, Pavia, Italy.
- Domaneschi, M. (2010), "Feasible control of the ASCE benchmark cable-stayed bridge", *Struct. Control Health*, **17**, 675-693.
- Domaneschi, M. and Martinelli, L. (2009), "Passive and semi-active seismic protection of the ASCE cable-stayed bridge", *Proc. of The Twelfth International Conference on Civil, Structural and Environmental Engineering Computing (CC2009)*, Funchal, Madeira, Portugal, 167.
- Domaneschi, M. and Martinelli, L. (2011), "Optimal passive and semi-active control of a wind excited suspension bridge", *Struct. Infrastruct. E.*, (in press). DOI: 10.1080/15732479.2010.542467.
- Domaneschi, M., Martinelli, L. and Romano, M. (2010), "A strategy for Modelling External User Element in ANSYS: the Bouc-Wen and the Skyhook case", *Proc. of 34th IABSE Symposium 2010*, Venice, Italy.
- Erlicher, S. and Point, N. (2004), "Thermodynamic admissibility of Bouc-Wen type hysteresis models", *CR Mecanique*, **332**(1), 51-57.
- Eurocode 8 (1998), UNI ENV 1998, *Design of structures for earthquake resistance*.
- Fogazzi, P. and Perotti, F. (2000), "The dynamic response of seabed anchored floating tunnels under seismic excitation", *Earthq. Eng. Struct. D.*, **29**(3), 273-295.
- Hague, S. (1997), "Composite design for long span bridges", *Proc. of the XV ASCE Structures Congress*, Portland, Oregon.
- Hong, A.L., Ubertini, F. and Betti, R. (2009), "Wind analysis of a suspension bridge: identification and FEM simulation", *J. Struct. Eng.-ASCE.*, **137**(1).
- Ikhouane, F., Manosa, V. and Rodellar, J. (2005), "Adaptive control of a hysteretic structural system", *Automatica*, **41**(2), 225-231.
- Ikhouane, F., Manosa, V. and Rodellar, J. (2007), "Dynamic properties of the hysteretic Bouc-Wen model", *Syst. Control Lett.*, **56**(3), 197-205.
- Low, T.S. and Guo, W. (1995), "Modeling of a three-layer piezoelectric bimorph beam with hysteresis", *J. Microelectromech. S.*, **4**(4), 230-237.
- Luco, J.E. and Wong, H.L. (1986), "Response of a rigid foundation to a spatially random ground motion", *Earthq. Eng. Struct. D.*, **14**(6), 891-908.
- MATLAB, R. (2008b), The MathWorks Inc., Natick, MA.
- Martinelli, L., Barbella, G. and Feriani, A. (2011), "A numerical procedure for simulating the multi-support seismic response of submerged floating tunnels anchored by cables", *Eng. Struct.*, **33**(10), 2850-2860.
- Monti, G., Nuti, C. and Pinto, P.E. (1996), "Nonlinear response of bridges under multisupport excitation", *J. Struct. Eng.-ASCE*, **122**(10), 1147-1159.
- Oppenheim, A.V. and Shafer, R.W. (2010), *Discrete-time Signal Processing*, Prentice Hall, ISBN-13: 978-0-13-198842-2.
- Shinozuka, M. (1972), "Monte carlo solution of structural dynamics", *Comput. Struct.*, **10**, 855-874.
- Sieffert, J.G. and Cevaer, F. (1992), *Handbook of Impedance Function*, Ouest Editions, Presses Academiques. ISBN 2-908261-32-4.

- Spencer, B.F. Jr, Dyke, S.J., Sain, M.K. and Carlson, J.D. (1997), "Phenomenological model for magnetorheological dampers", *J. Eng. Mech.-ASCE*, **123**(3), 230-238.
- Spencer, B.F. Jr and Nagarajaiah, S. (2003), "State of the art of structural control", *J. Struct. Eng.-ASCE*, **129**(7), 845-856.
- Ubertini, F. and Domaneschi, M. (2006), "Analytic and numeric approach to controlled cables", *Proc. of GIMC2006*, Univ. di Bologna, Bologna, Italy. ISBN 88-371-1621-7.
- Wen, Y.K. (1976), "Method for random vibration of hysteretic systems", *J. Eng. Mech.-ASCE, Div-ASCE*, **102**(2), 249-263.

SA